Volume 1 | Number 1 | Jan 2013 | Pages 1–100

PCCP

Physical Chemistry Chemical Physics
www.rsc.org/pccp

ROYAL SOCIETY OF CHEMISTRY

ROYAL SOCIETY OF CHEMISTRY

www.rsc.org/pccp

Optimization of absorption bands of dye-sensitized and perovskite tandem solar cells based on loss-in-potential values.

Jan Sobuś [1,2] and Marcin Ziółek [2]*

[1] *NanoBioMedical Centre, Adam Mickiewicz University, Umultowska 85, 61-614 Poznan, Poland.*

[2] *Quantum Electronics Laboratory, Faculty of Physics, Adam Mickiewicz University, Umultowska 85, 61-614 Poznan, Poland.*

* corresponding author, email: marziol@amu.edu.pl

Physical Chemistry Chemical Physics Accepted Manuscript

Abstract

A numerical study of optimal bandgaps of light absorbers in tandem solar cell configurations are presented with the main focus on dye-sensitized solar cells (DSSC) and perovskite solar cells (PSC). The limits in efficiency and the expected improvements of tandem structures are investigated as a function of total loss-in-potential (V_L), incident photon to current efficiency (*IPCE*) and fill factor (*FF*) of individual components. It is shown that the optimal absorption onsets are significantly smaller than those derived for multi-junction devices. For example, for double-cell devices the onsets are at around 660 nm and 930 nm for DSSC with iodide based electrolytes and around 720 nm and 1100 nm for both DSSC with cobalt based electrolytes and PSC. Such configurations can increase total sunlight conversion efficiency by about 35 % in comparison to single-cell devices of the same V_L, *IPCE* and *FF*. The relevance of such studies for tandem n-p DSSC and for a proposed new configuration for PSC is discussed. In particular, it is shown that a maximum total losses of 1.7 V for DSSC and 1.4 V for tandem PSC are necessary to give any efficiency improvement with respect to the single bandgap device. This means, for example, that a tandem n-p DSSC with TiO_2 and NiO porous electrodes will hardly work better than champion single DSSC. A source code of the program used for calculations is also provided.

Introduction

So far, commercial photovoltaic market is dominated by crystalline Si and thin film solar cells. However, the cost of both technologies is still too high for widespread use of photovoltaics. In recent years a few novel, photovoltaic solutions have emerged using the latest advances in nanotechnology, like organic photovoltaics (OPV), dye-sensitized solar cells (DSSC), quantum dots solar cells (QDSC) and perovskite solar cells (PSC). They are expected to become low-cost alternatives to the crystalline inorganic semiconductors technologies. Within emerging photovoltaics the current laboratory record efficiencies (at standard sunlight conditions AM1.5) are: 15% for PSC,[1-3] 12.3% for DSSC,[4] 10.6% for OPV[5] and 7.0% for QDSC[6]. Despite a huge progress in recent years, these efficiencies are still not high enough to compete with crystalline inorganic semiconductor technology.[7]

Still, despite their inferior absolute efficiency, they have clear advantages when economical and environmental issues are taken into account. Due to the solution based processing technologies without need of elevated temperatures, energy input needed for production of $1m^2$ of module of the DSSC, PSC or OPV is lower by at least order of magnitude, compared to the crystalline inorganic semiconductor technologies. This leads to energy payback time (EPBT) shortened from the 6 months period for thin film PV, to 1 month for OPV, with predicted EPBT for solution processed PSCs in the range of days. Moreover, there is also present a great reduction of greenhouse gases emission, compared to the first and second generation cells (not to mention classical fossil fuels). With the lack of scarce and environmentally hazardous materials (lead in PSCs being the only notable exception) and predicted cost of around 0.2\$/W, significantly lower than 0.5-1\$/W offered by the best contemporary thin-film technologies - the OPV, DSSC and PSC offer a viable way to challenge the ever-growing energy demand of the future.[8, 9]

On the one hand, in order to improve the global efficiency of the cell, absorption onset of the photoactive material should be extended into the red part of the spectrum to increase the photocurrent (J_{SC}). On the other hand, an increase in absorption onset results also in decreased open circuit voltage (V_{OC}), and, accordingly, decreased global efficiency. Therefore, there is a certain optimum wavelength for absorption onset at which the efficiency reaches a maximum. In the crystalline inorganic semiconductor photovoltaics this is the main reason for the well-known Shockley-Queisser limit of sunlight conversion efficiency of the single-bandgap device, which is 31% for a bandgap of 1.31 eV (absorption onset at 950

nm).[10] Other numerical calculations give a limit of 33% for a bandgap of 1.34 eV (925 nm) for unfocused standard Sun spectrum at the Earth surface (AM1.5).[11, 12]

As was recently nicely shown by Snaith, this optimum onset is not valid for DSSC which possess large loss-in-voltage.[13] Certain driving forces are required to efficiently inject electrons, transport them through the nanoparticle network, and regenerate the dye by electrolyte (Figure 1A), so the *Voc* is always significantly lower than the difference in potentials of the ground and excited state of the dye (absorption bandgap). For iodide-based electrolyte the typical losses are about 0.75 V and the absorption onset was reported to be at 840 nm giving the maximum possible global efficiency of 13.4% (with fill factor 0.73 and incident photon to current efficiency 90%).[13] Interestingly, this is very close to the best reported laboratory efficiencies obtained for ruthenium-complex DSSC and iodide-based electrolyte (11.2% for N719 [14] and 11.7% for C106 dye [15], both with absorption onset at 800 nm). This example emphasises that for the champion cells with iodide electrolyte the quantum yields of charge transfer processes are almost optimised and, without changing the electrolyte, not much of further improvement can be achieved.

The idea of tandem structures was successfully used in crystalline silicon and GaAs photovoltaic devices in the so called third generation of solar cells based on multi-junction systems.[16, 17] It is based on separating the absorption of the polychromatic solar spectrum into materials with different bandgaps. High energy photons are absorbed by the high bandgap junction and lower energy photons are absorbed at the lower bandgap, which allows a large portion of the solar spectrum to be absorbed while decreasing thermalization losses from carriers relaxing to the conduction band minimum. With this concept, the Shockley-Queisser limit of the efficiency of single-bandgap device can be overcome. Indeed, the current record sunlight conversion efficiency is 44 % for a three-junction solar cell.[7]

Among emerging photovoltaics, it is only organic solar cells technology in which the tandem structure recently resulted in the improvements of record efficiency (10.6 % [5]) with respect to that of a single device (9.2% [18]). In OPV a strong limitation is the maximum width of absorption bandgap in polymers, so the better efficiency in tandem structure is mainly due to extension of absorption range. For DSSC and QDSC the best tandem structures still have lower sunlight conversion efficiencies that their single-cell counterparts.
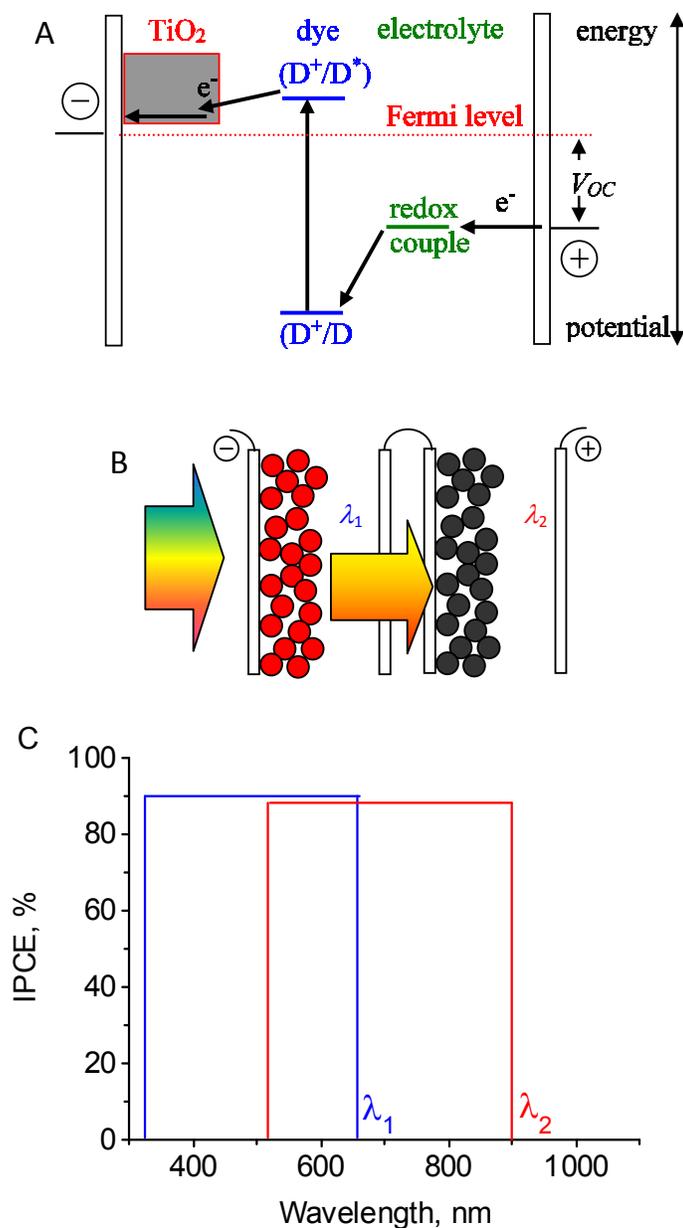
Figure 1. Schemes of DSSC energetics (A), simplest tandem cell connected in series (B) and idealized IPCE spectra for double bandgap tandem cell (C).

We think that one of the main factors that limit the successful use of tandem concept in emerging photovoltaics progress is the lack of proper adjustment of absorption onsets of the building absorber components. Due to certain differences with respect to classical crystalline inorganic semiconductor cells, mainly much larger loss-in-potential, the results obtained for multi-junction devices cannot be directly applied for OPV, DSSC and QDSC. Therefore, new calculations for these devices are necessary, which are the subject of this

contribution. As shown above and discussed in recent papers, loss-in-potential is a simple but very useful parameter to estimate the possible global performance of photovoltaic devices.[13, 19, 20] In this work we extend this model towards tandem structures of solar cell. We mainly focus on the discussion of DSSC and PSC, but the studies are also relevant for the improvement of other photovoltaic devices, like OPV and QDSC.

Methods

The global efficiency (η) of a solar cell is calculated as:

$$\eta = \frac{J_{sc}\, V_{oc}\, FF}{P_{in}}, \tag{1}$$

where FF is fill factor of the cell, and P_{in} is the irradiance of the light, which for standard AM 1.5 conditions (at Earth's surface) equals to 100 mW cm^{-2}. J_{sc} is related to the incident photon to current efficiency ($IPCE$) which describes the probability of conversion of one incident photon at a given wavelength to one electron, in the following way:

$$J_{SC} = \int_{\lambda_0}^{\lambda_{onset}} IPCE(\lambda)\, e\, \varphi_{ph}(\lambda)\, d\lambda, \tag{2}$$

where e is the elementary charge, φ_{ph} is the photon flux (at AM 1.5 conditions), λ_{onset} is the absorption onset (long-wavelength limit of the active material or dye absorption band), and λ_0 is the starting wavelength for sunlight spectrum (λ_0=300 nm, below that value the amount of photons is negligible from photovoltaic point of view). AM1.5 spectrum was taken from ASTM G173-03 reference spectra (hemispherical tilted 37 degrees).[21] V_{OC} is the difference between the maximum possible potential due to energy bandgap and internal loss-in-potential V_L:

$$V_{oc} = \frac{1240}{\lambda_{onset}\,[\text{nm}]} - V_L \text{ (in Volts)}. \tag{3}$$

For example, for DSSC, V_{OC} is the difference (Figure 1A) between the Fermi level in the semiconductor nanoparticles (close to the bottom edge of their conduction band) and the redox potential of the redox pair in the electrolyte. Therefore, in our calculations for a single device, the λ_{onset} parameter is varied for given V_{loss}, FF and $IPCE$ values, the efficiencies are calculated from eq. (1) to (3), and the best one is found. It is similar to the procedure used previously.[13]

6

Absorption onset λ_{onset} is the parameter that can be experimentally measured in IPCE spectra. In most cases it can be directly related to the active material bandgap: E_g [eV]$=1240/\lambda_{onset}$[nm]. However, in some configurations of DSSC the electron injection from hot excited state of the dye can be more efficient than that from the relaxed state (when the latter lies below TiO_2 conduction band). In that case the absorption onset from IPCE spectra corresponds to higher energy than the dye absorption bandgap.

For tandem structures a series connection of the building sub-cells is assumed since it is usually easier for technical implementation (Figure 1B). Therefore, the current-matching conditions should be fulfilled for the optimized configuration:

$$J_{SC} = \int_{\lambda_0}^{\lambda_1} IPCE_1(\lambda)\, e\, \varphi_{ph}(\lambda)\, d\lambda = \int_{\lambda_0}^{\lambda_2} IPCE_2(\lambda)\, e\, \varphi_{ph}(\lambda)\, d\lambda = ... = \int_{\lambda_0}^{\lambda_n} IPCE_n(\lambda)\, e\, \varphi_{ph}(\lambda)\, d\lambda \,, (4)$$

where λ_1, λ_2 …, λ_n are the absorption onsets of the materials in each parts ($\lambda_1 < \lambda_2 < ... < \lambda_n$). If the currents are not matched, then the smallest photocurrent of those achieved in each of particular n sub-cells is the one that occurs in the whole tandem device. The total V_{OC} of the device is the sum of open circuit voltages in each parts:

$$V_{oc} = \left(\frac{1240}{\lambda_1 \text{ [nm]}} - V_{L1} \right) + \left(\frac{1240}{\lambda_2 \text{ [nm]}} - V_{L2} \right) + ... + \left(\frac{1240}{\lambda_n \text{ [nm]}} - V_{Ln} \right), \qquad (5)$$

where V_{L1}, …, V_{Ln} are loss-in-voltages in each part of tandem device. Therefore, searching for optimized configuration is realized by scanning absorption onsets and calculating efficiencies from eq. (1), (4) and (5). In the first approximation, the idealized rectangular shapes of IPCE spectra are considered (Figure 1C). Then, more realistic shapes without steep onsets are taken into account. All the calculations were performed with the program, which code (in C++) can be downloaded as supporting material. The supporting information contains also more detailed description of how the program works.

Results and discussion

3.1. Initial considerations

Unless stated otherwise, all the results below will be presented for a fixed value of FF=0.73 for the whole tandem cell and maximum value of IPCE spectrum equal 90% in all parts of tandem cell, for the consistency with the previous studies for single cells.[13] These values are target parameters for good solar cells. If FF or both $IPCE$ are different from these

7

values (but the same in all parts) it will only proportionally affect the global efficiency of the device, not the optimized absorption onsets.

At the beginning, we assume that IPCE spectra have steep onsets (Figure 1C). For constant relations between IPCE in each sub-cell there is a constant relation between absorption onsets of each part: λ_1 , λ_2 …, λ_n. It is a direct consequence of current matching condition (eq. (4)). Figure 2 presents these relations for up to $n=5$ tandem cells as a function of the most short-wavelength onset of the first part of tandem cell, λ_1. These calculations are performed assuming that *IPCE* amplitudes of each part are the same and none of the incident photons from one part of the cell matching its IPCE spectrum is transferred to the proceeding part. Thus, if λ_1 is given for certain loss-in-potential, the rest of absorption onsets are automatically determined (and can be taken from Figure 2).
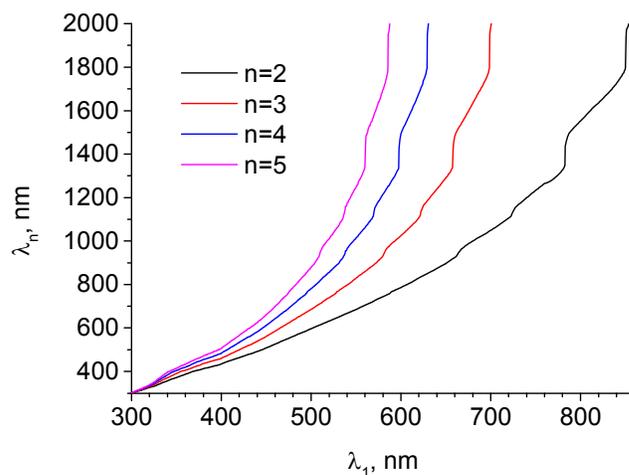

Figure 2. The dependence of the sub-cell absorption onsets on the onset of the first compartment for $n=2$, $n=3$, $n=4$ or $n=5$ tandem cells for perfect current matching conditions. The calculations are done assuming that *IPCE* amplitudes of each part are the same and none of the incident photons from one part of the cell matching its IPCE spectrum is transferred to the proceeding part.

Next, as comes from eq. (5), only the total loss-in-potential of all parts can be considered as varying parameter: $V_{LT}=V_{L1}+V_{L2}+…+V_{Ln}$. This means that for tandem solar cell performance, it is not important if losses are higher in one part and smaller in another, as long as their sum remains constant. It has a significant practical implementation – a tandem system can consist of the parts in which different driving forces (and thus losses in available voltage) are necessary for effective charge separation. Therefore the energy levels can be tuned in one

of the "weak" sub-cells to keep *IPCE* values high enough to maintain current-matching conditions.

We will present and discuss the cases of 3 different representative values of loss-in-potential, V_L. The efficiencies in corresponding tandem cells consisting of *n* parts, where the total loss-in-potential is assumed to be $V_{LT} = n \ V_L$, are shown. The first, highest value is $V_L = 0.75$ V which corresponds to DSSC with iodide/iodine electrolyte.[13] In this system the major contribution to the loss-in-potential is the high difference between the redox potentials of the dye and I_3^-/I^- redox couple, necessary for efficient dye regeneration. Nevertheless, the systems with ruthenium dyes and iodide-based electrolytes still keep the best certified DSSC efficiencies. Similar loss-in-potential of 0.75-0.80 V is given by the best OPV devices.[18, 20] Next, V_L=0.60 V is considered, which corresponds to Co-complex based electrolyte. It is one-electron redox shuttle which requires less reduction/oxidation steps in regeneration process and has redox potential shifted positively by about 0.2 V with respect to iodide/triiodide.[4, 22] Therefore, a gain of at least 0.15 V can be expected. Although the best DSSC laboratory efficiency is reported ~~just~~ for cobalt-based electrolyte,[4] it suffers from fast recombination and, so far, only works well with a specially designed dyes that block the access of redox couple to titania surface. Finally, the best and the lowest loss-in-potential values of 0.45 V correspond to organometal halide perovskite solar cells.[20] It is very recent and rapidly developing kind of solar cells with the active material exhibiting remarkable absorption and charge transport properties.[1, 2, 20, 23, 24] As it has been shown recently, the low loss-in-potential of PSC is approaching the best values of GaAs (below 0.3 V) and crystalline Si or CIGS solar cells (around 0.4 V).[20] The calculations for other loss-in-potentials can be easily obtained with the help of the attached program.

Finally, it should be noted that our simulations are not relevant for the systems when more than one absorbing material interacts with the same electrode. For example, in DSSC this is the case for co-sensitized dyes on nanoparticles, additional dyes interacting through Fourier Resonance Energy Transfer or making stacking nanoparticle layers sensitized with different dyes.[25-28] In many cases such structures have yielded better overall efficiencies of the solar cell (including the current champion DSSC with porphyrin dyes[4]) due to the extension of overall absorption range and are also often called tandem structures. However, they yield one photovoltage determined by the smallest bandgap absorber and cannot take full advantage of multi-bandgap concept (decreasing thermalisation losses). The optimization of absorption bandgaps of all contributors of such system should be done by matching the total absorbance

to the best absorption range of single device with the loss-in-potential of the smallest bandgap absorber.

3.2. Calculations for idealized model

The calculated best efficiencies for single cell are η=14.3% for V_L=0.75 V (with λ_{onset}=812 nm), η=17.6% for V_L=0.60 V (with λ_{onset}=892 nm) and η=20.6% for V_L=0.45 V (with λ_{onset}=896 nm). They can be used as reference for tandem devices. It can be noted that our optimum absorption onset and efficiency for V_L=0.75 V (812 nm, 14.3%) are slightly different from that reported previously (η=13.4% and λ_{onset}=840 nm).[13] The possible reason is that in the previous calculations a rise in IPCE to occur over 50 nm from the absorption onset was considered and the integration of photons from sunlight spectrum started from 400 nm, while in our case we start from 300 nm, see eq. (2).

An interesting feature is that the optimum onsets for V_L=0.60 V and V_L=0.45 V are almost the same (892 and 896 nm). This is because in the AM1.5 spectrum there is a huge gap from 890 to 990 nm due to the absorption of water vapors in the atmosphere. Therefore, the current gain due to the absorption red-shift is very small, and losses smaller than 0.25 V are necessary to "skip" this gap for the compensation of V_{OC} decrease. Indeed, when we made a control optimization with the assumed unreal photon flux spectrum without the gap (Figure S1), then the absorption onset were at 890 nm for V_L=0.60 V and 990 nm for V_L=0.45 V. This feature of sunlight spectrum at Earth surface has quite important practical implications. For example, it indicates that one does not need materials with absorption onset within the discussed gap because either λ_{onset} up to 900 and or λ_{onset} above 990 nm are optimal, depending on V_L.

This and other gaps in sunlight spectrum have implications also in the optimized wavelengths of the tandem devices. Figure 3 presents the comparison of efficiencies of tandem devices with V_L=0.75 V, V_L=0.60 V and V_L=0.45 V with respect to the absorption onset of the first sub-cell, λ_1. Double-cell devices are shown in part A, while Figure 3B and 3C show the results for n=3 and n=4, respectively. Several "saw-like" features in the curves are due to the above-mentioned gaps. The corresponding absorption onsets for the rest of compartments, λ_i (i=2,3,4) can be found from Figure 2. The best efficiencies and the corresponding optimized absorption onsets are also collected in Table 1. For example, for the simplest n=2 tandem device the best efficiencies are: η=19.8% for V_L=0.75 V (with λ_1=661 nm and λ_2=929 nm), η=23.6% for V_L=0.60 V (with λ_1=716 nm and λ_2=1096 nm), and

10

η=27.9% for V_L=0.45 V (with λ_1=718 nm and λ_2=1110 nm). Again, there is hardly any difference in the optimized onsets for V_L=0.60 V and V_L=0.45 V due to the water-vapor absorption gap in sunlight spectrum. The best efficiencies are better by a factor of about 1.36 with respect to those of single devices. Further increase of sub-cells number does not provide such significant improvements: it is only additional factor of 1.15 for n=3 and extra factor of 1.07 for n=4 (see Table 1). As expected, the trend in absorption onsets is similar to that reported already for single solar cells – the wavelength are shorter with increasing loss-in-potential.[13]

Table 1.

The best efficiencies (η) and the corresponding optimized absorption onsets (λ_i) for the indicated number of sub-cells (n) and loss-in-potential (V_L) in single sub-cell. The total loss-in-potential is assumed to be $V_{LT}= n\ V_L$.

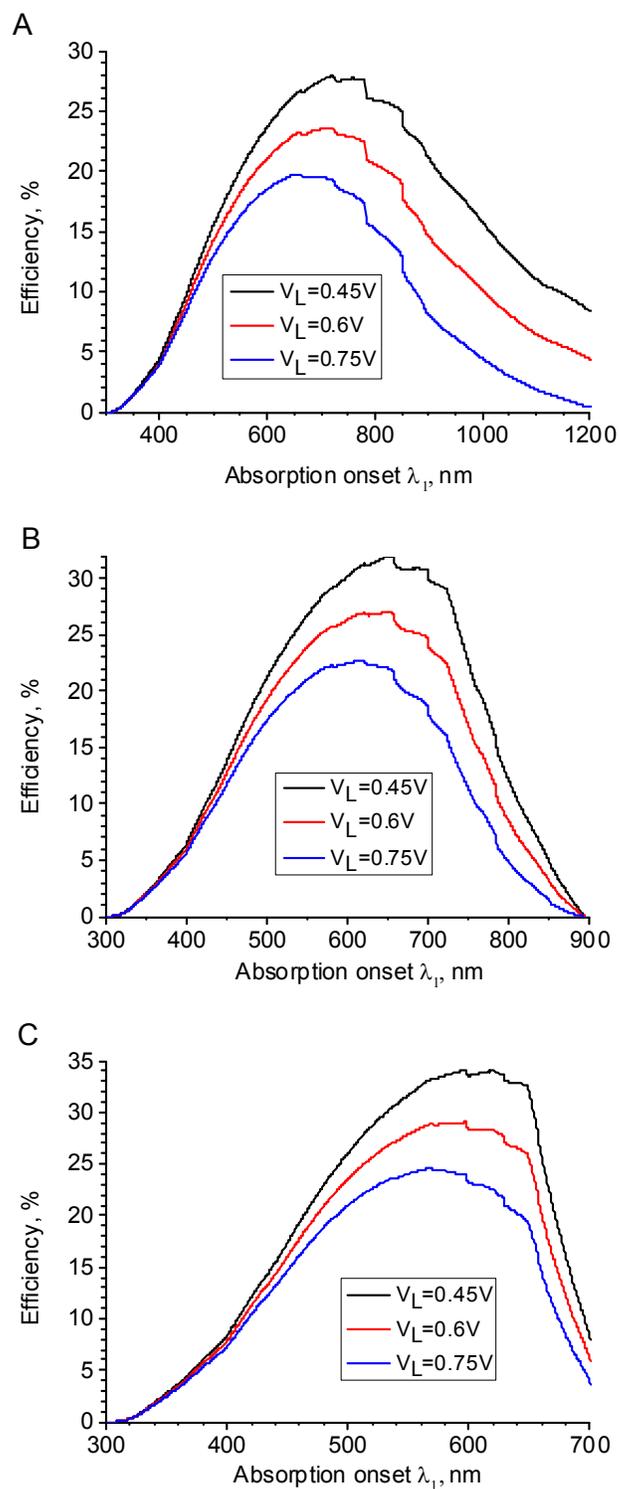|	V_L =0.75 V	V_L =0.60 V	V_L =0.45 V
n=1	η=14.3% λ_1=812 nm	η=17.6% λ_1=892 nm	η=20.6% λ_1=896 nm
n=2	η=19.8% λ_1=661 nm λ_2=929 nm	η=23.6% λ_1=716 nm λ_2=1095 nm	η=27.9% λ_1=718 nm λ_2=1100 nm
n=3	η=22.7% λ_1=616 nm λ_2=820 nm λ_3=1088 nm	η=27.0% λ_1=650 nm λ_2=895 nm λ_3=1287 nm	η=32.0% λ_1=655 nm λ_2=911 nm λ_3=1319 nm
n=4	η=24.6% λ_1=568 nm λ_2=720 nm λ_3=885 nm λ_4=1105 nm	η=29.1% λ_1=597 nm λ_2=780 nm λ_3=1013 nm λ_4=1330 nm	η=34.1% λ_1=597 nm λ_2=780 nm λ_3=1013 nm λ_4=1330 nm

Figure 3.

Comparison of efficiencies of tandem devices with different loss-in-potential as a function of

the absorption onset of the first sub-cell for *n*=2 (A), *n*=3 (B) and *n*=4 (C).

The values collected in Table 1 can be compared with those for multi-junction solar cells. The studies of maximum possible efficiencies are well established and have been calculated with different thermodynamic approaches or detailed balance theory.[29] The corresponding bandgaps for such devices have been calculated using either analytical or numerical sunlight spectrum.[11, 12, 29] For updated AM1.5 non-concentrated spectrum and series connection they are: 1.60 eV (λ_1=775 nm) and 0.94 eV (λ_2=1320 nm) for 2-junction solar cells (giving maximum efficiency of 46%), and 1.90 eV (λ_1=653 nm), 1.37 eV (λ_1=905 nm) and 0.94 eV (λ_3=1320 nm) for 3-junction solar cells (giving maximum efficiency of 52%).[11] However, the optimized absorption onsets are the target values only for GaAs and Si devices, which possess low internal voltage losses. As shown in our calculations, these values are not relevant for realistic tandem cells of novel photovoltaic systems (like DSSC, OPV, QDSC, PSC), for which the absorption onsets are shifted towards shorter wavelength.

Recently, it has also been shown that for the multi-junction inorganic semiconductor solar cells the optimum bandgaps depend on the quality and luminescence efficiency of the material.[30, 31] With increasing nonradiative recombination in the material (and, thus, decreasing luminescence quantum yield) the bandgaps should be lowered, the trend similar to the one obtained in our calculations. The luminescence efficiency was related to the open circuit voltage of the solar cell. [32] However, in the case of DSSC and PSC the luminescence properties of the absorbing material have lower impact on the maximum photovoltage. It is because charge transport is realized in other components than those absorbing the light. Therefore, the main contribution to loss-in-voltage comes from the driving forces necessary for both efficient electron and hole separations at interfaces, for example electron injection and dye regeneration for DSSC.

Several tandem DSSC structures using two separate cells were investigated with the cell of shorter absorption onset facing the Sun.[33-38] It seems that in many previous attempts to build efficient tandem cells the optimized conditions were not fully realized. Quite often a "good" dye was taken for the first cell (having significant efficiency and absorbing up to 800 nm) and then another dye, absorbing more to the red, was added to the second unit, left with insufficient sunlight to achieve similar photocurrent. It also does not make sense to look for dyes for DSSC absorbing further in NIR than up to 930 nm for iodide based electrolytes. For cobalt-based electrolytes (or perovskites) the materials do not need to have absorption beyond 1100 nm for double-band tandem cells. For the first compartment of the tandem DSSC, dyes with absorption onsets around 660 nm are best suited for iodide based electrolytes. This

13

means that a lot of "forgotten" dyes that did not give high efficiencies in single devices (but had high maximum of IPCE spectra) can be reinvestigated for tandem application. On the other hand, if a dye for a second compartment does not absorb sufficiently far in the red, than it is better to optimize the absorption onset of the first dye towards even shorter wavelength (close to 600 nm) to fulfill the matching current condition. The same situation applies if a second sub-cell has IPCE spectrum of much lower values than those of the first sub-cell. We will come back to these issues in sections 3.4 and 3.5 below.

3.3. Combined n-p type tandem configurations

A significant challenge in tandem configurations is the way of making the efficient optical and electrical connection between the sub-cells. Completely separate units (like the ones schematically presented in Figure 1B) are rather expensive, for example due to the additional costs of electrodes. In multi-junction solar cells the connection between different compartments is realized through tunnel junctions, however this approach is both expensive and not possible for fabrication with novel solar cells discussed here. In tandem QDSC and OPV recombination layers are used.[39, 40] For DSSC, other approaches like floating electrode for bottom cell[41] or integrated tandem cells[42] have also been proposed.

However, tandem configuration of double DSSC can be realized in intuitively elegant and potentially cheap combined n-p DSSC.[43] Its scheme is shown in Figure 4A. The n-type part is the photoanode used in the classical DSSC, built of nanoparticle network of n-doped semiconductor (usually TiO_2) that collects and transports injected electrons. The p-type part is in many ways the reverse concept to the n-type one.[44] A porous material is placed on the counter electrode to collect and transport the injected holes. The holes (instead of electrons) are injected to the valence band (instead of conduction band) of a semiconductor (usually NiO) from the dyes attached with the electron withdrawing group to the nanoparticles' surfaces. The dyes are regenerated by the hole transfer from the redox pair in the electrolyte, the latter process being the equivalent of the redox pair oxidation on the counter electrode in classical DSSC. In the combined n- and p-type device, the same electrolyte is used to regenerate the dyes on n-type side.

The best efficiencies of p-type DSSC devices are still very low, up to 1.3%,[45] so n-p tandems also suffer from poor performance. The problem with p-type part is that significant driving forces are necessary (and, thus, large loss-in-potential) for obtaining reasonable IPCE values. For example, the systems with high IPCE require the blue-absorbing dye on the p-

part.[46] Therefore, it is reasonable to ask what is the limit of total loss-in-potential (V_{LT}) at which the maximum efficiency of the tandem device drops below the maximum efficiency of single device. Our calculations indicate (Figure 4C) that it is maintained for V_{LT} <2.0 V for iodide-based electrolytes and V_{LT} <1.7 V for cobalt-based electrolytes. Taking the optimized absorption onsets for such limiting systems we can calculate from eq. (5) that the minimum total V_{OC} of such system has to be 1.4 V for iodide DSSC and 1.6 V for cobalt DSSC. It should be noted that we refer to iodide- or cobalt- based electrolytes only in the context of target best efficiency of single device. In n-p DSSC device the type of redox couple used does not influence the total V_{OC} - it can only modify IPCE spectra of both n- and p- components.

Note that the differences between the potential of conduction band edge of TiO_2 (about -0.5 V vs. NHE) and valence band edge of NiO (about 0.6 V vs. NHE) is the maximum V_{OC} available from such tandem device (Figure 4A) and it is only about 1.1 V. This means that a tandem n-p DSSC made with TiO_2 and NiO will hardly give the expected better efficiency than a champion single DSSC device. Our calculations indicate that in order to maintain V_{OC} as small as 1.1 V and have the best efficiency above 19% (to beat a single cobalt-based DSSC with best η=17.6%, see Table 1) one needs a very unrealistic total loss-in-potential of $V_{LT}=V_{L1}+V_{L2}$=1.3 V and absorption onset of the second dye as far as λ_2=1500 nm. We think that it is quite important conclusion which suggests that it is better to work on the photocathodes with semiconductors of much more positive potential of the valence bandgap than NiO. $CuAlO_2$ and $CuGaO_2$ have potentials by about 0.2 V more positive with respect to NiO, which puts them on the similar best possible efficiency as single DSSC. Better improvement can be reached with $CuGaO_2$ which valance band energy is further 0.2 eV lower.[47] In such conditions both V_{LT} can be higher and λ_2 can be smaller to maintain best efficiency above 19%.

According to our knowledge, tandem structures of perovskites solar cell have not been reported so far. Therefore, we would like to propose a possible compact configuration of such tandem device based on the n-p concept of DSSC (Figure 4B). It should be noted that it uses perovskites material for both sub-cells. The proposed configuration takes the advantage of perovskite material that is a very good electron and hole transporter.[24] Indeed, it has been reported for efficient PSC that electron transporting TiO_2 material can be substituted with Al_2O_3 and electrons are efficiently transported through perovskite material itself.[48] Similarly, quite efficient PSC without any additional hole transporting material was built.[49] Therefore, two perovskite mesoporous layers with optimized absorption onsets can substitute both

sensitizing dye and charge transporting mesoporous semiconductor layer, and it can work on photoanode (perovskite "n") as well as on photocathode (perovskite "p"). Hole transporting material (HTM, for example spiro-OMeTAD) can act as analogue to redox couple in n-p DSSC. The maximum possible V_{OC} would be the difference between the potential of conduction band edge of perovskite "n" and valence band edge of perovskite "p".
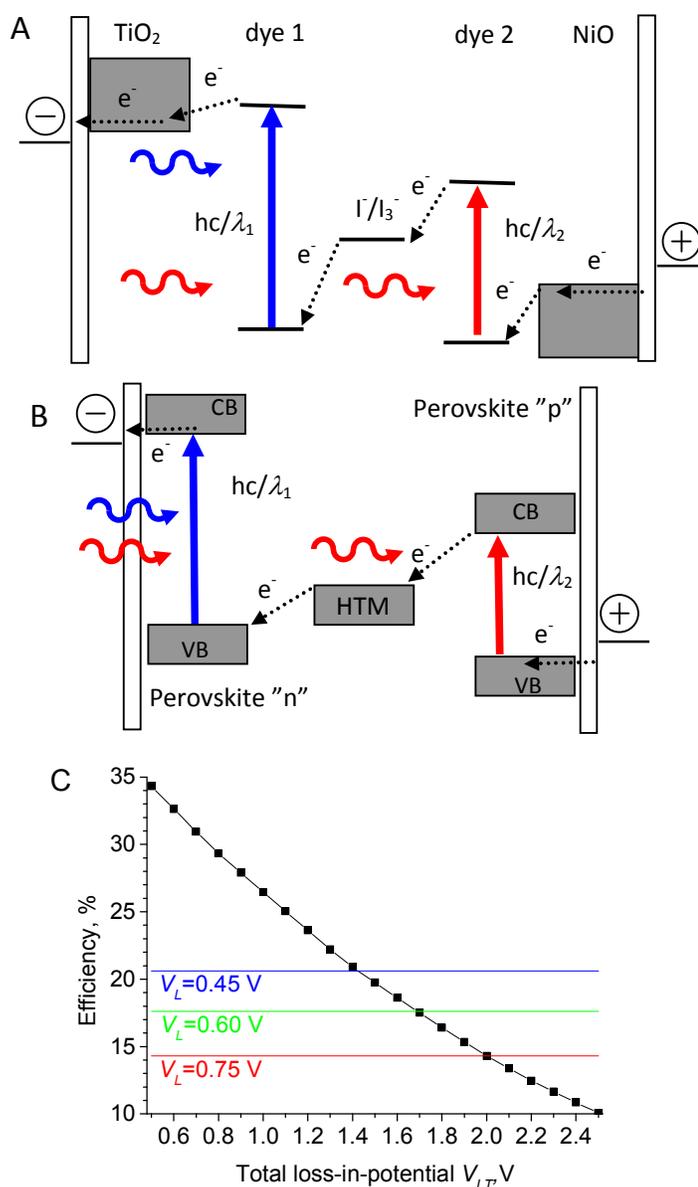

Figure 4. Scheme of n- and p- type tandem DSSC (A) and a proposed new structure of tandem perovskite solar cell (B). The best efficiency as a function of total loss-in-potential for a tandem cell with 2 sub-cells, $n=2$ (C). The horizontal lines indicate the best efficiencies of single devices for indicated V_L corresponding to PSC (V_L=0.45 V), cobalt-based DSSC (V_L=0.60 V) and iodide-based DSSC (V_L=0.75 V).

16

Due to the lower loss-in-potential of PSC the conditions for tandem n-p perovskite configuration are even more rigorous than for DSSC. According to our calculations, the total loss in potential has to be V_{LT} <1.4 V for such tandem configuration to give better efficiency than a single device with V_L =0.45 V (Figure 4C). This means that a potential of valence band of perovskite "p" has to lie significantly below HOMO level of HTM. Such modification can be quite challenging within organometal halide perovskites used so far. All the reported modifications that result in lowering valence band led to simultaneous increase in conduction band energy when atoms of higher electronegativity are used. For example, the valence band edge of $CH_3NH_3PbBr_3$ is 0.14 eV below that of $CH_3NH_3PbI_3$, but at the same time the bandgap increases from 1.5 to 2.2 eV.[50] In this way, the loss-in-potential for electron transfer to HTM would be too high. Therefore, probably new types of perovskites are necessary for such tandem devices.

3.4. Optimization limits

We would like to discuss the limits in which the absorption onset can be changed without significant alteration of the global efficiency (up to 10% relative change). The example will be discussed for n=2 and iodide-based DSSC. The crucial role of current matching condition should be emphasised, which is even more important than the long enough absorption onset of the dyes. For example, if the long-wavelength onset is shifted by 100 nm (from λ_2=929 to λ_2=829 nm) and the short-wavelength one is shifted accordingly to keep the optimum matching (from λ_1=661 nm down to λ_1=620 nm) then the tandem maximum efficiency does not drop so much: from 19.8% to 19.1% (with V_{L1}=V_{L2}=0.75 V), which is only 4% relative change. However, if λ_1 stays fixed at 661 nm and we move only λ_2, much bigger losses occur (gathered in the Figure 5). It is visible immediately that too short λ_2 is more harmful (reaching 10% relative efficiency loss with absorption shift of around $\Delta\lambda_2$=-40nm), while for too long λ_2 the loss is significantly lower ($\Delta\lambda_2$ of around 140 nm needed for 10% relative efficiency loss).

These results, presented in Figure 5, can be explained by the balance between I_{SC} and V_{OC} in equation (1). Below optimal cutoff, the voltage of the second junction is higher, but its current is lower than the one of the first junction and it effectively becomes I_{sc}, lowering efficiency of the entire device. Thus, for example, if we cannot get sufficiently red-absorbing material for a second sub-cell of tandem DSSC, it is better to shift the absorption of the first sub-cell towards shorter wavelength to maintain current matching conditions. In the too long

regime, however, the I_{sc} stays constant (being the lower current on the first junction, which remains unchanged). The only part that gets lowered is the voltage of the second sub-cell which decays as $1/\lambda_2$ (resulting V_{OC}=0.37+1240/λ_2). That means that the global efficiency loss of 10% will be met when V_{OC} will drop to 90% of initial value, which happens at λ_2=1070 nm. In fact, as long as 1240/λ_2 is higher than 0.75 V, the V_{LI} of the second junction, the tandem cell will be more efficient than a single one with given offset λ_1. It holds true for λ_2 up to 1650 nm.
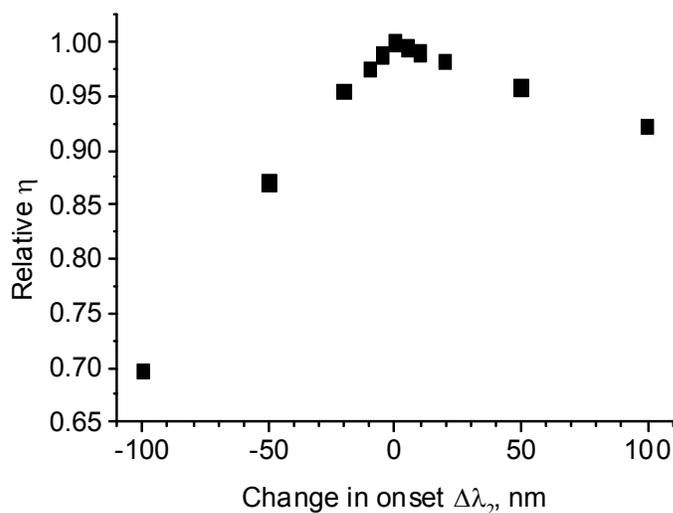

Figure 5. Relative loss in global efficiency of the tandem cell with fixed λ_1 and λ_2 shifted by $\Delta\lambda_2$ from optimized position.

When we fix λ_2 at optimum 929 nm and change λ_1, the situation is reversed. Moving λ_1 towards shorter wavelengths results in λ_2 too far in the red and slow decrease in performance, while moving λ_1 towards longer wavelengths makes λ_2 too short for optimal matching resulting in the more rapid loss. Therefore, moving λ_1 can be explained in terms of previous example. One can take new optimal λ_2 for the moved λ_1 from Figure 2, and then again treat λ_1 as a fixed parameter, with $\Delta\lambda_2$ equal to the difference between fixed λ_2 and optimal λ_2 from Figure 2 (with the base efficiency for given λ_1 taken form Figure 3). In both cases, loses from the onsets lying too close to each other are 3-4 times higher than in the situation when they are lying too far, for the same mismatch amplitude concerned.

3.5. Gradually rising IPCE spectra

Finally, we would like to discuss the influence of more realistic shapes of IPCE spectra and simulate the results for a couple of already reported tandem configurations.

First thing taken into account in this chapter is the fact that real IPCE spectra do not end instantly, but decay (usually in a gauss fashion) with some half-width. We checked the effect of this blur for single and double cells with the initial cutoff lengths optimized and V_L=0.75V (λ_1=812 nm for n=1 and λ_1=661 nm λ_2=929 nm for n=2). The IPCE spectra were fixed, so that half of maximum amplitude lies always at the wavelengths mentioned before. Gaussian decay was generated using expression (6) with λ_d tweaked so that half of the amplitude is fixed at one wavelength and A being maximum amplitude of IPCE.

$$IPCE(\lambda) = A\exp\left(-\frac{(\lambda-\lambda_d)^2}{2\sigma^2}\right) \tag{6}$$

Starting with σ=0 nm (square) up to σ=200 nm the IPCE curves are presented as insets in Figures 6A and 6B for n=1 and n=2 respectively. When calculating efficiency two situations were considered, taking absorption onset at half amplitude (keeping it constant independently of σ) and taking absorption onset at wavelength with 10% of initial amplitude. The first case (constant absorption onset λ_{onset} at half amplitude of IPCE) corresponds to the situation when for $\lambda>\lambda_{onset}$ smaller absorption gap ($1240/\lambda$) is compensated by loss-in-potential smaller then optimum, keeping ($1240/\lambda - V_L$) value constant. Therefore, the rise of IPCE is due to insufficient driving force and quantum yields of primary charge separation process (for example electron injection in DSSC). On the contrary, the case of keeping absorption onset at 10% of rising IPCE corresponds to the situation when a finite rise in IPCE is due to the insufficient absorption of the light, for example due to too thin absorption layer.

Obtained relative efficiencies (compared to σ=0) can be seen on Figures 6A and 6B for n=1 and n=2 respectively. It can be clearly observed that for both cells the blur has hardly any effect on the efficiency when the absorption onset is kept at a constant value (only change in I_{sc} would contribute here, but the current fluctuation is less than 3% up to σ=100 nm). This means that all our previous considerations based on ideal rectangle-like IPCE spectra (Figure 1C) on are also valid in this case.

With the moving onsets resulting in diminishing V_{oc}, one can see corresponding efficiency loss. Surprisingly, the loss scales fairly linearly in this region with about 10% loss in relative performance at σ=50 nm for single cell and σ=45 nm for tandem cell. This

convenient fact yields a nice method of estimation of maximum efficiencies of single and tandem devices, with the knowledge of IPCE spectra.
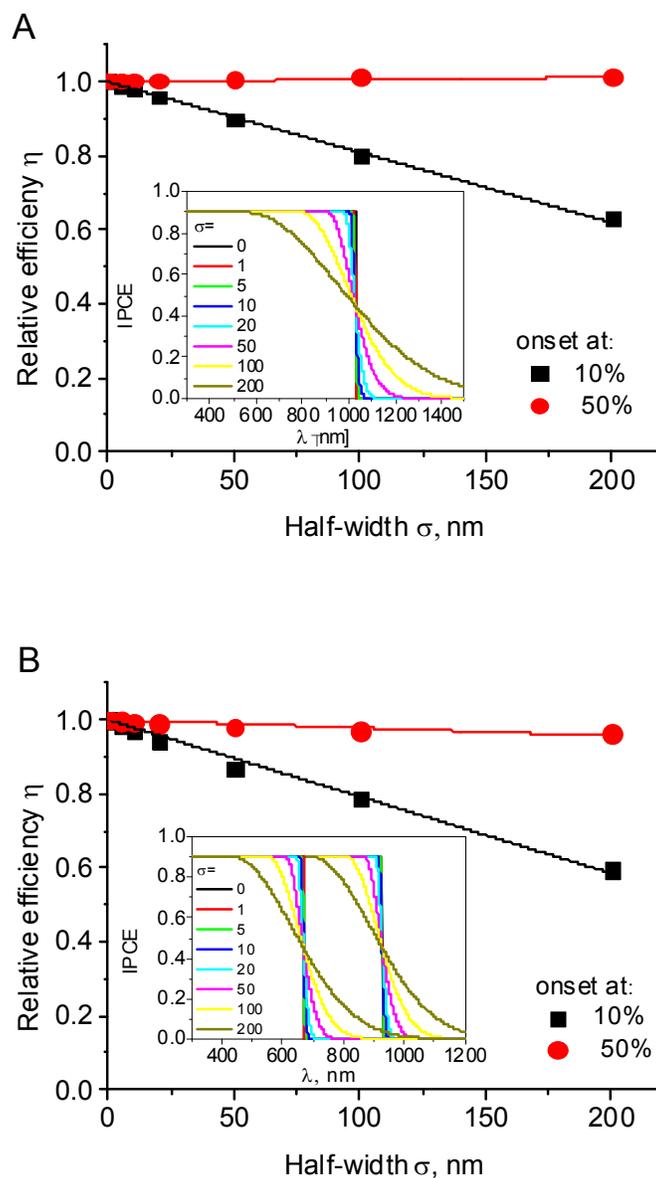

Figure 6. Relative loss in global efficiency of the tandem cell with fixed λ_1 and λ_2 with the changing half-width σ for single cell (A) and tandem cell (B). The absorption onset is set either at 50% or at 10% of IPVE curve. The insets show IPCE curves for given σ.

So far we assumed that maxima of IPCE spectra of all tandem components have the same value (90%). Our procedure and provided program also enables the calculation in the

cases when IPCE maxima are different, i.e. due to lower charge separation yields in some compartments. As expected, in these cases the optimized absorption onset might be different to those shown above. For example, for $n=2$ and iodide DSSC ($V_L=0.75$ V) we checked rather extreme case of $IPCE_1=90\%$ and $IPCE_2=50\%$ of rectangular shape. The obtained best efficiency was equal to 16.2% with absorption onsets at $\lambda_1=632$ nm and $\lambda_2=1096$ nm. Therefore, compared to the case of the same intensity of IPCE (Table 1), the onset of the first compartment is shifted to shorter, while that of the second compartment – to longer wavelength. When the values of IPCE intensity were exchanged ($IPCE_1=50\%$, $IPCE_2=90\%$ and assuming that no light within the IPCE spectrum of the first sub-cell passes to the second one), the situation is reversed: optimized onsets are at $\lambda_1=715$ nm (red shifted) and $\lambda_2=896$ nm (blue shifted). However, in this case the efficiency is only 12.7%, which is smaller than that of single device (14.3%, Table 1).

Finally, we would like to present the example of using our procedure to check the performance and suggest the way of improving of real tandem DSSC cell. We have chosen a recently reported tandem configuration with one of the best efficiencies reported so far (11.4%) utilizing novel DX1 dye and traditional sensitizer N719.[38] The IPCE spectra provided in this contribution were digitized and used as inputs in the program. Calculations yielded data that corresponded well with values reported by the authors: $I_{sc}=11.3$ mAcm^{-2}, $V_{oc}=1.46$V and $\eta=11\%$ when absorption onsets were taken at wavelengths corresponding to 10% of maximum IPCE amplitude (712 nm and 940 nm for top and bottom cell respectively). Simulation shows a little mismatch of the currents (11.3 mAcm^{-2} for top and 13.3 mAcm^{-2} for the bottom cell), but generally results are representing experimental data, with less than 10% error. Looking at the Table 1 one can see that the λ_2 of DX1 dye lies close to the optimal theoretical wavelength for the tandem system with iodide electrolyte – 929 nm. The λ_1, however, is lying too far to the red, lowering the total efficiency. Hence, we performed more simulations leaving bottom cell IPCE spectrum and FF intact, while taking the IPCE of the top cell as rectangle of height 0.7 spanning from 300 nm to the varying λ_1. It turned out that the maximum efficiency of 13.5% is achieved when the λ_1 is taken at 650 nm with $I_{sc}=11.7$ mAcm^{-2} and $V_{oc}=1.72$V. When we consider that there are dyes with IPCE ending within region of 600-650 nm which can achieve uniform IPCE of 0.9 amplitude, global efficiency can be pushed even higher. When the height of the top cell rectangular spectrum is set to 0.9 the simulated efficiency can reach 16.1% with the $\lambda_1=623$ nm, $I_{sc}=13.2$ mAcm^{-2} and $V_{oc}=1.81$ V.

Therefore, as alternatives to N719 some triphenylamine dyes with more blue shifted absorption onset can be proposed for the tandem configuration with DX1 dye. For example, TPC1[51] and TH305[52] dyes have high IPCE values and the time-resolved studies with our contribution confirmed high electron injection and dye regeneration quantum yields of these systems.[53, 54] DSSC with TPC1 dye has flat IPCE spectrum of 80-90% extending up to 530 nm with gradual decay up to 630 nm, while that with TH305 has IPCE spectrum shifted further to the red by 70 nm. Another alternative can be very recently introduced RK1 dye, having similar IPCE onsets to that of TH305 but yielding even better efficiencies.[55]

Conclusions

Loss-in-potential, V_L, of the solar cell (being the difference of the energy bandgap of active material and open circuit voltage of the cell) is a simple parameter that can help simulating the behavior of different photovoltaic devices. In this contribution we use this parameter to calculate the optimal absorption onsets of tandem DSSC and perovskite solar cells. Based on the proposed procedure and provided program, a number of results relevant for better optimization of such devices are shown and discussed.

For ideal case of rectangle IPCE spectra (with steep onset) the following optimal onsets and sunlight conversion efficiencies are obtained for tandem configurations with two sub-cells (assuming maximum IPCE value 90% and FF=0.73): λ_1=661 nm, λ_2=929 nm and η=19.8% for iodide-based DSSC (V_L=0.75 V), λ_1=716 nm, λ_2=1096 nm and η=23.6% for cobalt-based DSSC (V_L=0.60 V), and λ_1=718 nm, λ_2=1110 nm and η=27.9% for perovskite solar cells (V_L=0.45 V). Such configurations can increase the total sunlight conversion efficiency by about 35 % in comparison to the single-cell devices. It is shown that if the materials with optimized wavelengths are not available, it is better to vary the absorption onsets of all compartments to fulfill the current matching conditions than keeping one onset at fixed optimized position and vary other onsets. For more realistic IPCE curves (with Gaussian rise) the results do not depend on the width of spectral rise if absorption onsets are kept the same. If absorption onsets change according to the width of IPCE rise, then the sunlight conversion efficiency decreases linearly with a relative drop of about 20% of initial value per 100 nm width increase.

A novel configuration for tandem perovskite solar cell is proposed based on tandem n-p DSSC device. The conditions at which both of such tandem devices can be superior with respect to single solar cells is investigated. It is revealed that the sum of both loss-in-

potentials in n-p DSSC cannot exceed 1.7 V. Due to large potential losses of typical n-p DSSC with TiO_2 and NiO mesoporous films, such configurations will hardly provide better sunlight conversion efficiency than a single DSSC, therefore alternatives to NiO material with more positive potential of valence band should be explored. For tandem perovskites cells the conditions are even more rigorous and the total loss in potential has to be smaller than 1.4 V. This implies the need of new types of perovskites with more positive valence band potential.

Finally, the example of real IPCE spectra of functioning DSSC tandem device was used for calculation and discussion of the best absorption onsets. The provided procedure and program enables calculation of optimal absorption bandgaps and efficiencies for any given configuration of tandem solar cell and assumed loss-in-potential.

Electronic Supplementary Information (ESI) available:: Code (in C) for the program for predicting sunlight conversion efficiency (*code.c*). Sunlight spectrum (*AM15ext.txt*) and exemplary IPCE file for rectangle-like shape (*ipce1.txt*). Description of the program for optimizing bandgaps, figure S1 (*pdf* file).

Acknowledgements

References

1.   J. Burschka, N. Pellet, S.-J. Moon, R. Humphry-Baker, P. Gao, M. K. Nazeeruddin and M. Grätzel, *Nature*, 2013, **499**, 316-319

2.   M. Liu, M. B. Johnston and H. J. Snaith, *Nature*, 2013, **501**, 395-398.

3.   H.-S. Kim, S. H. Im and N.-G. Park, *J. Phys. Chem. C*, 2014, **118**, 5615-5625.

4.   A. Yella, H.-W. Lee, H. N. Tsao, C. Yi, A. K. Chandiran, M. K. Nazeeruddin, E. W.-G. Diau, C.-Y. Yeh, S. M. Zakeeruddin and M. Grätzel, *Science*, 2011, **334**, 629-634.

5.   J. You, L. Dou, K. Yoshimura, T. Kato, K. Ohya, T. Moriarty, K. Emery, C.-C. Chen, J. Gao, G. Li and Y. Yang, *Nat. Commun.*, 2013, **4**, 1446.

6.   A. H. Ip, S. M. Thon, S. Hoogland, O. Voznyy, D. Zhitomirsky, R. Debnath, L. Levina, L. R. Rollny, G. H. Carey, A. Fischer, K. W. Kemp, I. J. Kramer, Z. Ning, A.

J. Labelle, K. W. Chou, A. Amassian and E. H. Sargent, *Nature Nanotechnology*, 2012, **7**, 577-582.

7.   www.nrel.gov/ncpv, National Renewable Energy Laboratory (NREL)

8.   D. Yue, P. Khatav, F. You and S. B. Darling, *Energy Environ. Sci.*, 2012, **5**, 9163-9172.

9.   S. B. Darling and F. You, *RSC Adv.*, 2013, **3**, 17633-17648.

10.   W. Shockley and H. J. Queisser, *J. Appl. Phys.*, 1961, **32**, 510-519.

11.   S. P. Bremner, M. Y. Levy and C. B. Honsberg, *Prog. Photovolt: Res. Appl.*, 2008, **16**, 225–233.

12.   A. S. Brown and M. A. Green, *Physica E*, 2002, **14**, 96-100.

13.   H. J. Snaith, *Adv. Func. Mater.*, 2010, **20**, 13-19.

14.   M. K. Nazeeruddin, F. De Angelis, S. Fantacci, A. Selloni, G. Viscardi, P. Liska, S. Ito, B. Takeru and M. Grätzel, *J. Am. Chem. Soc.*, 2005, **127**, 16835-16847.

15.   Q. Yu, Y. Wang, Z. Yi, N. Zu, J. Zhang, M. Zhang and P. Wang, *ACS Nano*, 2010, **4**, 6032-6038.

16.   G. Conibeer, *Mater. Today*, 2007, **10**, 42-50.

17.   L. C. Hirst and N. J. Ekins-Daukes, *Prog. Photovolt: Res. Appl.*, 2011, **19**, 286-293.

18.   Z. He, C. Zhong, S. Su, M. Xu, H. Wu and Y. Cao, *Nature Photonics*, 2012, **6**, 591-595.

19.   B. E. Hardin, H. J. Snaith and M. D. McGehee, *Nature Photonics*, 2012, **6**, 162-169.

20.   H. J. Snaith, *J. Phys. Chem. Lett.*, 2013, **4**, 3623-3630.

21.   http://rredc.nrel.gov/solar/spectra/am1.5/ASTMG173/ASTMG173.html.

22.   S. M. Feldt, E. A. Gibson, E. Gabrielsson, L. Sun, G. Boschloo and A. Hagfeldt, *J. Am. Chem. Soc.*, 2010, **132**, 16714-16724.

23.   N. G. Park, *J. Phys. Chem. Lett.*, 2013, **4**, 2423-2429.

24.   S. D. Stranks, G. E. Eperon, G. Grancini, C. Menelaou, M. J. P. Alcocer, T. Leijtens, L. M. Herz, A. Petrozza and H. J. Snaith, *Science*, 2013, **342**, 341-344.

25.   B. E. Hardin, E. T. Hoke, P. B. Armstrong, J. H. Yum, P. Comte, T. Torres, J. M. J. Fréchet, M. K. Nazeeruddin, M. Grätzel and M. D. McGehee, *Nature Photonics*, 2009, **3**, 406-411.

26.   S. K. Balasingam, M. Lee, M. G. Kang and Y. Jun, *Chem. Comm.*, 2013, **49**, 1471-1487.

27. Y. Ogomi, S. S. Pandey, S. Kimura and S. Hayase, *Thin Solid Films*, 2010, **519**, 1087-1092.

28. M. Cheng, X. Yang, J. Li, F. Zhang and L. Sun, *ChemSusChem*, 2013, **6**, 70-77.

29. A. Martí and G. L. Araújo, *Sol. Energy Mater Sol. Cells*, 1996, **43**, 203-222.

30. N. L. A. Chan, N. J. Ekins-Daukes, J. G. J. Adams, M. P. Lumb, M. Gonzalez, P. P. Jenkins, I. Vurgaftman, J. R. Meyer and R. J. Walters, *IEEE J. Photovoltaics*, 2012, **2**, 202-208.

31. T. P. White, N. N. Lal and K. R. Catchpole, *IEEE J. Photovoltaics*, 2014, **4**, 208-214.

32. G. Smestad and H. Ries, *Sol. Energy Mater Sol. Cells*, 1992, **25**, 51-71.

33. W. Kubo, A. Sakamoto, T. Kitamura, Y. Wada and S. Yanagida, *J. Photochem. Photobiol. A: Chem*, 2004, **164**, 33-39.

34. M. Dürr, A. Bamedi, A. Yasuda and G. Nelles, *Appl. Phys. Lett.*, 2004, **84**, 3397-3399.

35. M. Yanagida, N. Onozawa-Komatsuzaki, M. Kurashige, K. Sayama and H. Sugihara, *Sol. Energy Mater Sol. Cells*, 2010, **94**, 297-302.

36. L. Li, Y. Hao, X. Yang, J. Zhao, H. Tian, C. Teng, A. Hagfeldt and L. Sun, *ChemSusChem*, 2011, **4**, 609-612.

37. D. Xiong and W. Chen, *Front. Optoelectron.*, 2012, **5**, 371-389.

38. T. Kinoshita, J. T. Dy, S. Uchida, T. Kubo and H. Segawa, *Nature Photonics*, 2013, **7**, 535-539.

39. X. Wang, G. I. Koleilat, J. Tang, H. Liu, I. J. Kramer, R. Debnath, L. Brzozowski, D. A. R. Barkhouse, L. Levina, S. Hoogland and E. H. Sargent, *Nature Photonics*, 2011, **5**, 480-484.

40. T. Ameri, N. Li and C. J. Brabec, *Energy Environ. Sci.*, 2013, **6**, 2390-2413.

41. K. Uzaki, S. S. Pandey and S. Hayase, *J. Photochem. Photobiol. A: Chem*, 2010, **216**, 104-109.

42. R. Tagliaferro, D. Gentilini, S. Mastroianni, A. Zampetti, A. Gagliardi, T. M. Brown, A. Reale and A. Di Carlo, *RSC Adv.*, 2013, **3**, 20273-20280.

43. A. Hagfeldt, G. Boschloo, L. Sun, L. Kloo and H. Pettersson, *Chem. Rev.*, 2010, **110**, 6595-6663.

44. J. He, H. Lindström, A. Hagfeldt and S. E. Lindquist, *J. Phys. Chem. B*, 1999, **103**, 8940-8943.

45. S. Powar, T. Daeneke, M. T. Ma, D. Fu, N. W. Duffy, G. Götz, M. Weidelener, A. Mishra, P. Bäuerle, L. Spiccia and U. Bach, *Angew. Chem.*, 2013, **125**, 630-633.

46. A. Nattestad, A. J. Mozer, M. K. R. Fischer, Y.-B. Cheng, A. Mishra, P. Bäuerle and U. Bach, *Nature Mater.*, 2009, **9**, 31-35.

47. M. Yu, T. Draskovic and Y. Wu, *Phys. Chem. Chem. Phys.*, 2014, **16**, 5026-5033.

48. M. M. Lee, J. Teuscher, T. Miyasaka, T. N. Murakami and H. J. Snaith, *Science*, 2012, **338**, 643-647.

49. W. A. Laban and L. Etgar, *Energy Environ. Sci.*, 2013, **6**, 3249-3253.

50. J. H. Noh, S. H. Im, J. H. Heo, T. N. Mandal and S. I. Seok, *Nano Lett.*, 2013, **13**, 1764-1769.

51. H. Tian, X. Yang, R. Chen, R. Zhang, A. Hagfeldt and L. Sun, *J. Phys. Chem. C*, 2008, **112**, 11023-11033.

52. H. Tian, X. Yang, J. Cong, R. Chen, J. Liu, Y. Hao, A. Hagfeldt and L. Sun, *Chem. Comm.*, 2009, 6288-6290.

53. M. Ziółek, B. Cohen, X. Yang, L. Sun, M. Paulose, O. K. Varghese, C. A. Grimes and A. Douhal, *Phys. Chem. Chem. Phys.*, 2012, **14**, 2816-2831.

54. M. Ziółek, C. Martín, L. Sun and A. Douhal, *J. Phys. Chem. C*, 2012, **116**, 26227-26238.

55. D. Joly, L. Pelleja, S. Narbey, F. Oswald, J. Chiron, J. N. Clifford, E. Palomares and R. Demadrille, *Sci. Rep.*, 2014, **4**, 4033.

Graphical abstract

The dependence of best sunlight conversion efficiency and optimum absorption onset of the first sub-cell on the loss-in-potential (V_L) and number of sub-cells in tandem solar cells.